ELSEVIER

Composites: Part A 33 (2002) 155–161

composites
Part A: applied science and manufacturing

www.elsevier.com/locate/compositesa

Manufacturing theory for advanced grid stiffened structures

Steven M. Huybrechts*, Troy E. Meink, Peter M. Wegner, Jeff M. Ganley

Air Force Research Laboratory, Space Vehicles Directorate, AFRL/VSSV, 3550 Aberdeen Ave SE, Kirtland AFB, NM 87117-5776, USA

Received 22 December 1999; revised 28 June 2001; accepted 29 June 2001

Abstract

Lattices of rigidly connected ribs, known as *advanced grid stiffened* (AGS) structures, have many advantages over traditional construction methods, which use panels, sandwich cores and/or expensive frameworks. The technology behind these structures has progressed significantly during the past five years to the point where these structures are being integrated into operational systems. Two tooling methods for fabricating these structures using composite materials have proven to be highly effective at achieving high quality, low cost AGS structures: the hybrid tooling method and the expansion block method. Both methods rely on a precise understanding of tooling behavior during cure to achieve proper consolidation, often determined through trial and error. This paper proposes a theory governing the behavior of both tooling types during the cure cycle in order to minimize the trial and error required to understand tooling expansion during cure. The theory is validated by experimental data. Published by Elsevier Science Ltd.

Keywords: E. Tooling; A. Tow; A. Fibres; Advanced grid stiffened structures

1. Introduction

1.1. Advanced grid stiffened structures

Advanced grid stiffened (AGS) structures, or grid structures, have long been of interest as a replacement for honeycomb sandwich and aluminum isogrid constructions but, for many decades, were unused due to the tremendous manufacturing and analysis challenges associated with their construction. During the past 10 years, remarkable progress has been made in the manufacturing and design of these structures. Programs at The Boeing Company, The US Air Force Research Laboratory, McDonnell-Douglas (now part of The Boeing Company), Alliant Tech Systems, Composite Optics International Inc., Stanford University, and others have pushed the state of the art in grid stiffened structures, finally leading to processes and methods of interest to real-world production systems. As a result, AGS structures have found their way into several business jets, research satellites and the Minotaur Launch Vehicle. Additionally, they are currently being investigated by a number of aerospace structure manufacturers.

Typically, AGS Structures are fabricated using continuous fiber organic composite materials. These structures are characterized by a shell structure (or skin) supported by a lattice pattern (or grid) of stiffeners. Typically, these stiffeners run in 2–4 directions along the shell forming a repeating pattern. Examples of these structures are shown in Fig. 1. A broad overview of AGS structures, their manufacture, design, and analysis is given in Ref. [1]. More detailed information can be found in Refs. [2–5].

All AGS structures suffer from the same manufacturing difficulty: for an AGS structure to have all fibers continuous through a rib crossing point, there must be twice as much material in each crossing point than in each rib, making rib compaction difficult or impossible. For most manufacturing methods, this difficulty leads to a buildup at the nodal points, which is undesirable for many reasons, including loss of strength, stiffness, and modeling accuracy.

Two types of tooling have proven to be effective in overcoming this problem: hybrid tooling and expansion block tooling. Both provide lateral compaction of the ribs during cure by taking advantage of the thermal expansion of the tooling material.

1.2. Hybrid tooling

The concept of hybrid tooling solves many of the problems associated with rib compaction while providing a number of additional advantages. Hybrid tooling offers an AGS structure manufacturing solution that is low cost, is highly automated, provides good part compaction and good geometry control. An example of hybrid tooling is shown in Fig. 2.

* Corresponding author. Tel.: +1-505-846-8253; fax: +1-505-846-7877.
E-mail address: steven.huybrechts@kirtland.af.mil (S.M. Huybrechts).

1359-835X/02/$ - see front matter Published by Elsevier Science Ltd.
PII: S1359-835X(01)00113-0

Report Documentation Page

Form Approved
OMB No. 0704-0188

Public reporting burden for the collection of information is estimated to average 1 hour per response, including the time for reviewing instructions, searching existing data sources, gathering and maintaining the data needed, and completing and reviewing the collection of information. Send comments regarding this burden estimate or any other aspect of this collection of information, including suggestions for reducing this burden, to Washington Headquarters Services, Directorate for Information Operations and Reports, 1215 Jefferson Davis Highway, Suite 1204, Arlington VA 22202-4302. Respondents should be aware that notwithstanding any other provision of law, no person shall be subject to a penalty for failing to comply with a collection of information if it does not display a currently valid OMB control number.

1. REPORT DATE **2002**	2. REPORT TYPE	3. DATES COVERED **-**
4. TITLE AND SUBTITLE **Manufacturing theory for advanced grid stiffened structures**		5a. CONTRACT NUMBER 5b. GRANT NUMBER 5c. PROGRAM ELEMENT NUMBER
6. AUTHOR(S) **Steven Huybrechts; Troy Meink; Peter Wegner; Jeff Ganley**		5d. PROJECT NUMBER 5e. TASK NUMBER 5f. WORK UNIT NUMBER
7. PERFORMING ORGANIZATION NAME(S) AND ADDRESS(ES) **Air Force Research Laboratory/VSSS,3550 Aberdeen Ave SE,Kirtland AFB,NM,87117-5776**		8. PERFORMING ORGANIZATION REPORT NUMBER
9. SPONSORING/MONITORING AGENCY NAME(S) AND ADDRESS(ES)		10. SPONSOR/MONITOR'S ACRONYM(S) 11. SPONSOR/MONITOR'S REPORT NUMBER(S)

12. DISTRIBUTION/AVAILABILITY STATEMENT
Approved for public release; distribution unlimited

13. SUPPLEMENTARY NOTES

14. ABSTRACT
Lattices of rigidly connected ribs, known as advanced grid stiffened (AGS) structures, have many advantages over traditional construction methods, which use panels, sandwich cores and/or expensive frameworks. The technology behind these structures has progressed significantly during the past five years to the point where these structures are being integrated into operational systems. Two tooling methods for fabricating these structures using composite materials have proven to be highly effective at achieving high quality, low cost AGS structures: the hybrid tooling method and the expansion block method. Both methods rely on a precise understanding of tooling behavior during cure to achieve proper consolidation, often determined through trial and error. This paper proposes a theory governing the behavior of both tooling types during the cure cycle in order to minimize the trial and error required to understand tooling expansion during cure. The theory is validated by experimental data.

15. SUBJECT TERMS

16. SECURITY CLASSIFICATION OF:			17. LIMITATION OF ABSTRACT	18. NUMBER OF PAGES	19a. NAME OF RESPONSIBLE PERSON
a. REPORT **unclassified**	b. ABSTRACT **unclassified**	c. THIS PAGE **unclassified**		**8**	

Standard Form 298 (Rev. 8-98)
Prescribed by ANSI Std Z39-18

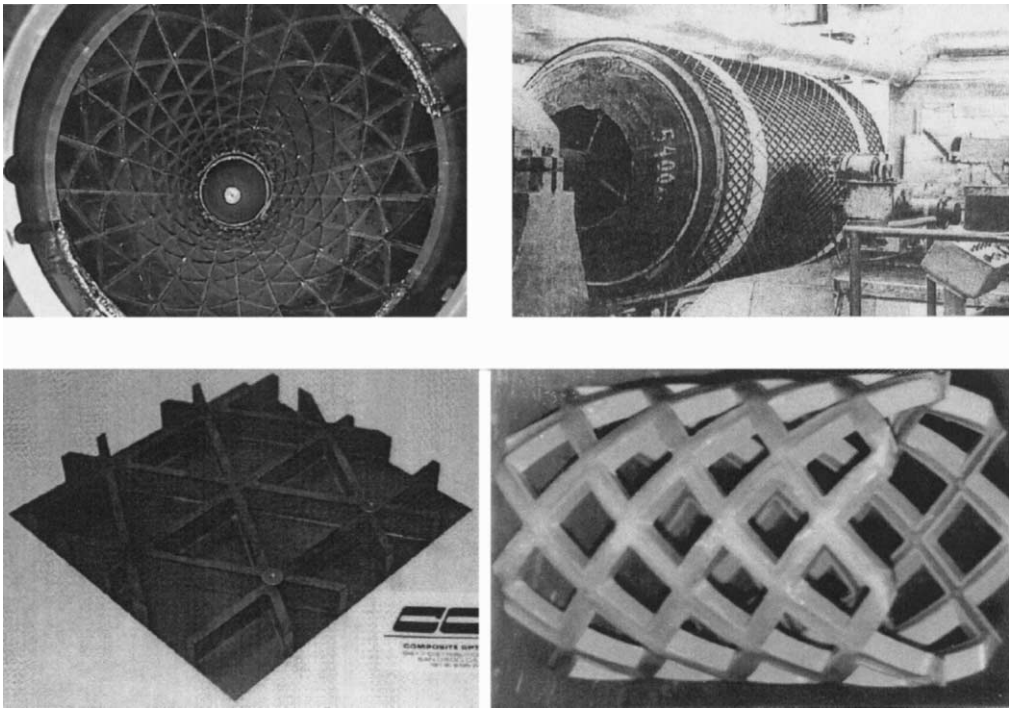

Fig. 1. Examples of AGS structures: (clockwise from top left) Air Force Research Laboratory's Payload shroud; Russian aircraft fuselage; COI's SnapSat technique for satellites; Stanford's TRIG structure.

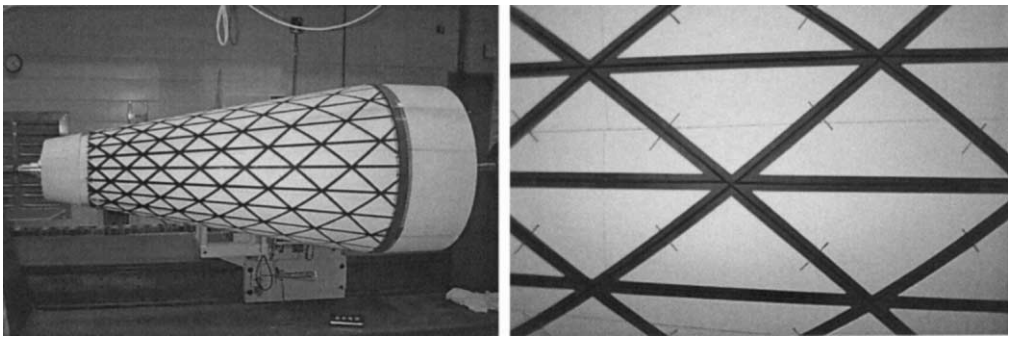

Fig. 2. Example of hybrid tooling: the base tool, in this case, is made of tooling epoxy and has grooves cut into it corresponding to the rib locations; the silicon rubber expansion tool is placed into these grooves.

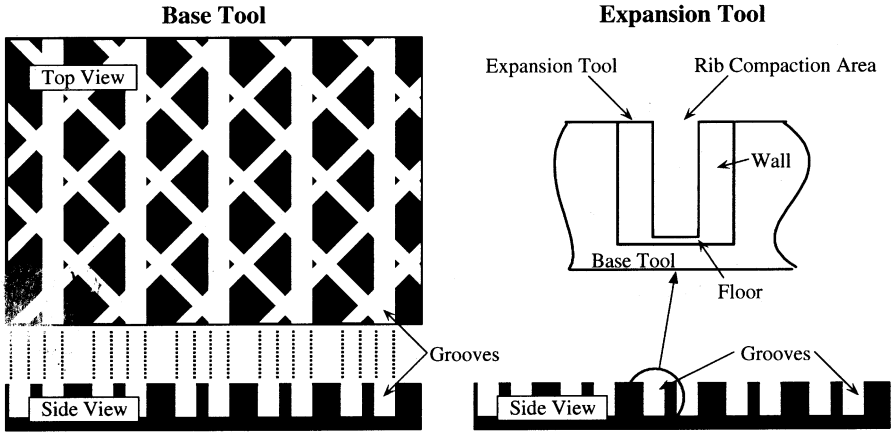

Fig. 3. Schematic of base and expansion tooling: hybrid tooling consists of a base and an expansion tool. The base tool is composed of a hard, thermally stable material with grooves cut into it. The expansion tool is composed of a high CTE material and is 'laid into' the base tool. Prepreg tow is laid or wound into the groove in the expansion tool to create the structure's ribs. A skin is then laid up or wound over the top of the base tool.

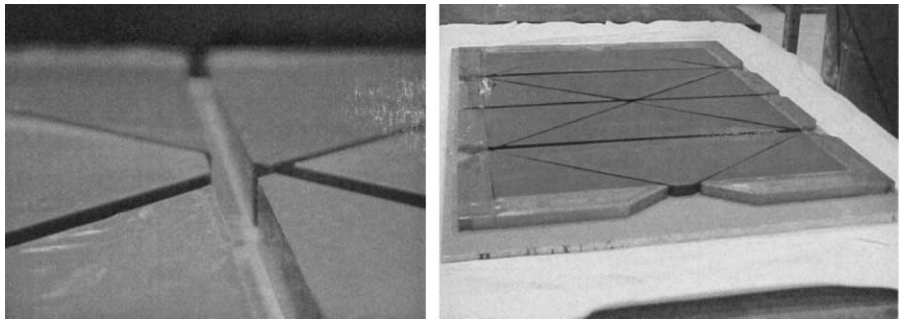

Fig. 4. Example of expansion block tooling: in this case, the base tool is made of aluminum, and the expansion blocks are cast silicon rubber.

Hybrid tooling uses two different tooling materials, one as a base tool and one as an expansion tool, combining the advantages and mitigating the disadvantages of each material. Grooves are machined into the base tool in which the expansion tool is placed. The expansion tool is typically a high thermal expansion material that is cast into channel sections. In this way, the base tool defines the shape of the part while the expansion tool provides lateral compaction to the ribs during cure. A schematic of the base and expansion tools is shown in Fig. 3.

1.3. Expansion block tooling

While hybrid tooling works well and is the tooling of choice in many cases, it is limited in the thickness of ribs it can produce due to the fact that the walls of the expansion tool become prohibitively wide. The concept of expansion block tooling, while more difficult in practice allows for a wider range of rib geometry. An example of expansion block tooling is shown in Fig. 4.

Expansion block tooling consists of a 'base tool', typically a stable, stiff material, and 'blocks' made of a nearly incompressible material having a high thermal expansion coefficient. During cure, the blocks expand to provide lateral compaction to the ribs. The block can be bolted to the base or simply placed against it. The ribs can be laid up before or after the blocks are placed depending on the process. A schematic of this tooling is shown in Fig. 5.

2. Theory

2.1. Rib sizing, compaction and imprinting

In order to achieve high quality parts using both hybrid and expansion block tooling, careful attention must be paid to sizing of the expansion tool or expansion blocks. When performing this sizing, minimization of imprinting must be considered. Imprinting is an undesired side effect of AGS tooling where the expansion tool/block causes impressions around the ribs or indentations at the ribs on the outside of the AGS structure skin. Additionally, the tooling must be sized so that the desired rib dimensions are achieved and so that the ribs are fully compacted.

2.2. Plane-strain hybrid tooling thermal model

A good intuition into the behavior of hybrid tooling can be gained from a closed form, plane strain solution. In this simple solution, the effect of the expansion tool floor is not considered. Additionally, it is assumed that the expansion of the base tool is much less than that of the expansion tool. This simplified situation is shown in Fig. 6.

Neglecting the effect of the expansion tool floor, there will be no shear deformation in the expansion tool and the constitutive equations will be [6, p. 22]

$$\begin{bmatrix} \varepsilon_x \\ \varepsilon_y \\ \varepsilon_z \end{bmatrix} = \frac{1}{E}\begin{bmatrix} 1 & -\nu & -\nu \\ -\nu & 1 & -\nu \\ -\nu & -\nu & 1 \end{bmatrix}\begin{bmatrix} \sigma_x \\ \sigma_y \\ \sigma_z \end{bmatrix} + \alpha\,\Delta T\begin{bmatrix} 1 \\ 1 \\ 1 \end{bmatrix} \quad (1)$$

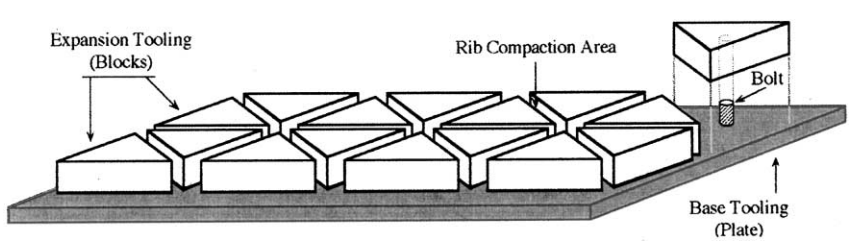

Fig. 5. Schematic of expansion block tooling: expansion block tooling consists of a stable base tool with expansion blocks.

where ε_i are the total strains in the i-direction, σ_i are the stresses in the i-direction, E, ν, α are the Young's modulus, Poisson's ratio, coefficient of thermal expansion of the expansion tool and ΔT is the change in temperature of the system. Solving for the plane strain condition yields

$$\varepsilon_x = \frac{1+\nu}{E}((1-\nu)\sigma_x - \nu\sigma_y + E\alpha\,\Delta T) \tag{2a}$$

$$\varepsilon_y = \frac{1+\nu}{E}(-\nu\sigma_x + (1-\nu)\sigma_y + E\alpha\,\Delta T) \tag{2b}$$

where the strain in the z-direction has been set to zero.

Assuming that during the cure cycle, the resin in the rib is in liquid form and that the expansion tool groove is sufficiently full of material to eliminate any membrane effect in the skin, the pressure on the top (y-direction) of the expansion tool and the uncured resin are both equal to the pressure being applied to the whole system. Due to the hydrostatic nature of liquids, the pressure applied laterally (x-direction) to the expansion tool is, therefore, also equal to the applied pressure. Therefore,

$$\begin{aligned} \sigma_x &= \sigma_y = -\sigma \\ \varepsilon_x &= \varepsilon_y = \varepsilon \end{aligned} \tag{3}$$

and the resulting constitutive equation for hybrid tooling and its inverse are

$$\begin{aligned} \varepsilon &= \frac{1+\nu}{E}((2\nu-1)\sigma + E\alpha\,\Delta T) \\ \sigma &= \frac{E}{2\nu-1}\left(\frac{\varepsilon}{1+\nu} - \alpha\,\Delta T\right) \end{aligned} \tag{4}$$

where σ is the applied pressure and ε is the hydrostatic strain in the expansion tool.

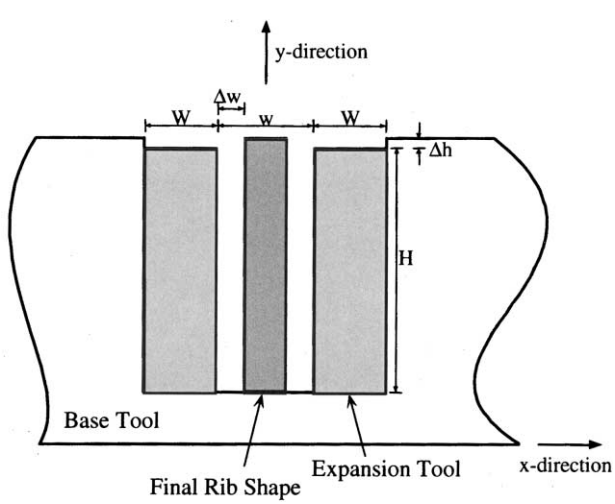

Fig. 6. Hybrid tooling thermal model diagram: the expansion tool expands Δw and Δh to compact the rib as shown. This thermal model neglects the effect of the expansion tool floor leading to a rectangular rib cross-section.

2.3. Expansion block tooling thermal model

A good intuition into the behavior of the expansion block tooling concept can be gained from a closed form, reduced 3D solution. In this simple solution, the effect of friction between the expansion blocks and the base tool as well as base tool expansion are not considered. The simplified situation is shown in Fig. 7.

Assuming no attachment of the expansion blocks or attachment to the base tool only at the center of expansion (the point where no lateral movement would have occurred had the block not been attached), there will be no shear deformation in the expansion tool and the constitutive equations will be [6, p. 22]

$$\begin{bmatrix} \varepsilon_x \\ \varepsilon_y \\ \varepsilon_z \end{bmatrix} = \frac{1}{E}\begin{bmatrix} 1 & -\nu & -\nu \\ -\nu & 1 & -\nu \\ -\nu & -\nu & 1 \end{bmatrix}\begin{bmatrix} \sigma_x \\ \sigma_y \\ \sigma_z \end{bmatrix} + \alpha\,\Delta T\begin{bmatrix} 1 \\ 1 \\ 1 \end{bmatrix} \tag{5}$$

where ε_i are the total strains in the i-direction, σ_i are the stresses in the i-direction, E, ν, α are as defined in Section 2.3. Assuming hydrostatic pressure on all sides of the block as discussed in Section 2.2,

$$\begin{aligned} \sigma_x &= \sigma_y = \sigma_z = -\sigma \\ \varepsilon_x &= \varepsilon_y = \varepsilon_z = \varepsilon \end{aligned} \tag{6}$$

the constitutive equation for expansion block tooling and its inverse reduce to

$$\begin{aligned} \varepsilon &= \frac{\sigma(2\nu-1)}{E} + \alpha\,\Delta T \\ \sigma &= \frac{E}{(2\nu-1)}(\varepsilon - \alpha\,\Delta T) \end{aligned} \tag{7}$$

where σ is the applied pressure and ε is the hydrostatic strain in the expansion block.

2.4. Using the hybrid tooling and expansion block tooling thermal models

Using the models developed in Section 2.2 and 2.3, it is possible to determine the required tooling geometry by assuming that the hydrostatic strain is determined by material curing requirements (applied pressure (σ) and cure temperature (ΔT)) and that the groove width (w) is determined by the desired rib geometry. An additional constraint, that the groove width must be equal to or wider than the prepreg tow width being used, is necessary to facilitate winding.

For either model (hybrid or expansion block), the hydrostatic strain in the expansion tool or expansion block can be written as

$$\varepsilon = \frac{\Delta h}{H} = \frac{\Delta w}{W} \tag{8}$$

where ε is defined in Eq. (4) or (7) depending on the tooling

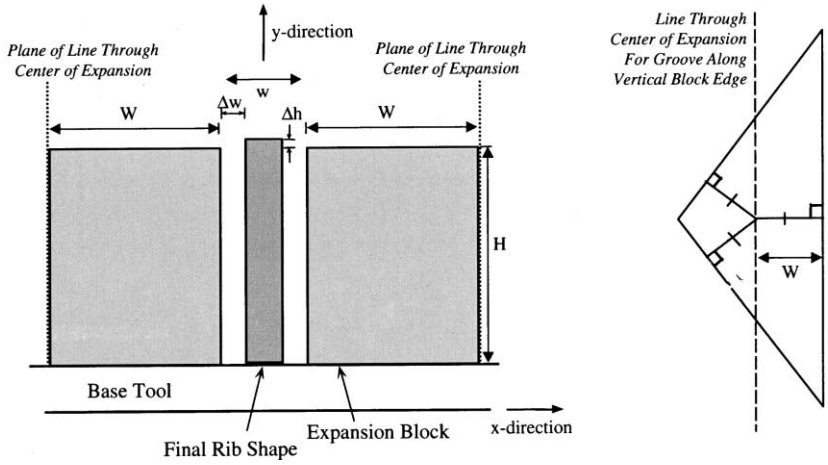

Fig. 7. Expansion block tooling thermal model diagram: the expansion block expands Δw and Δh to compact the rib as shown. W is taken from the plane of the line parallel to the block edge and through the center of expansion, the point of the block where the displacement after expansion is zero. For a triangle, this point is the median. An example is shown for the vertical (longest) edge of a triangular expansion block.

type being used (hybrid or expansion block). All other symbols in Eq. (8) are defined in Fig. 6 or 7, depending, again, on the tooling type used. For both tooling types, the desired rib width and rib height can be related to the tool geometry parameters through

$$R_h = H + \Delta h \tag{9}$$

$$R_w = w - 2\,\Delta w \tag{10}$$

where R_h and R_w are the desired rib height and width, respectively. Typically, for maximum flexibility, the groove width, w, is set close to its minimum possible value, the width of the prepreg tow being laid in the grooves. Considering w to be known, therefore, Eqs. (8)–(10) can be solved for the remaining expansion tool/block geometry parameters yielding

$$H = \frac{R_h}{1+\varepsilon} \tag{11}$$

$$\Delta h = H\varepsilon \tag{12}$$

$$W = \frac{w - R_w}{2\varepsilon} \tag{13}$$

$$\Delta w = W\varepsilon \tag{14}$$

where ε is a known parameter calculated from Eq. (4) or (7).

Finally, it is necessary to calculate the number of tows required to obtain the desired rib geometry. The number of pre-preg tows required is

$$T_n = \frac{R_w R_h}{T_A} \tag{15}$$

where T_A is the area of a single tow. Alternatively, substituting Eqs. (9), (10), (12), and (14) into Eq. (15) yields

$$T_n = \frac{H(w - 2W\varepsilon)(1+\varepsilon)}{T_A} \tag{16}$$

which must be satisfied in order to validate the assumption that there is no membrane effect in the skin, the requirement for the simplifications in Eqs. (3) and (6). A fractional number in Eq. (15) or (16) can be rounded off with minimal effect.

3. Experimental verification

3.1. Hybrid tooling model

To validate the model in Sections 2.2 and 2.4, several hybrid tool configurations were studied. In each case, the required number of tows was calculated using Eq. (16) and the hybrid tooling model of Section 2.2. Verification of the model was determined by comparing the experimentally achieved rib dimensions with those predicted by Eqs. (9) and (10).

The experimental setup is shown in Fig. 8. No skin was used so that the achieved rib height could be accurately determined. For each expansion tool configuration tested, the predicted number of tows, T_n, was laid up into the tool. The conditions were as follows: $\sigma = 620$ KPa, $E = 3.4$ MPa, $\nu = 0.482$, $\alpha = 2\times10^{-4}$ °C^{-1},

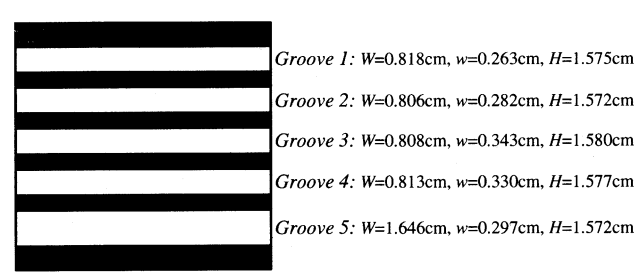

Fig. 8. Hybrid tooling thermal model test setup: the base tool material was tooling epoxy, and the expansion tool material was a high temperature silicon rubber.

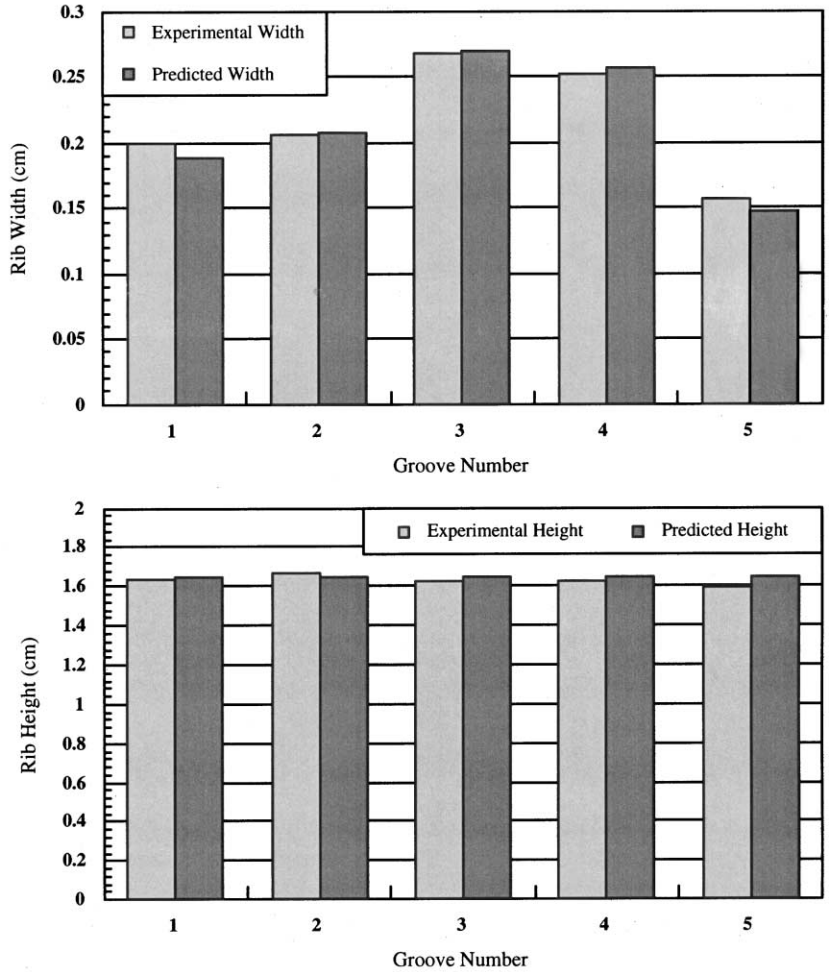

Fig. 9. Results of thermal model verification: the results of the thermal model verification are shown for an applied pressure of 620 KPa.

$\Delta T = 156°C$. The material used was IM7/977-2 and was cured to the manufacture's recommended cure cycle.

All results of the experiments were in good agreement with the model. The results obtained are shown in Fig. 9, where the experimental rib heights and widths are shown compared to those predicted by the theory. The largest difference between predicted and experimental dimensions was about 6% of the experimental rib width in that case.

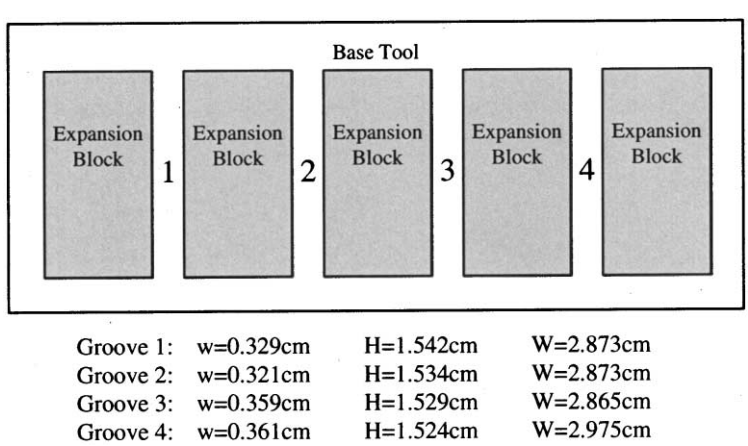

Fig. 10. Expansion block thermal model test setup: the base tool material was monolithic graphite, and the expansion block material was TFM1600, a modified teflon.

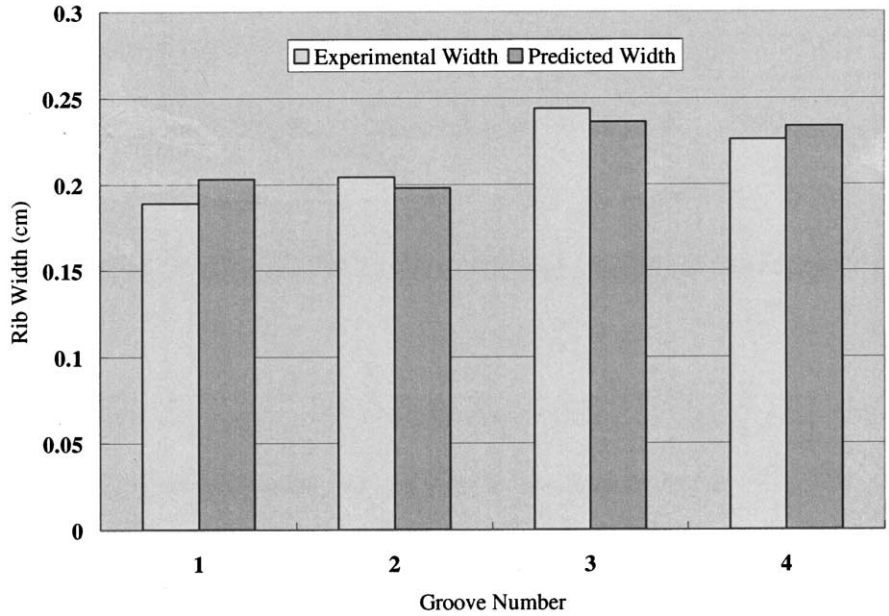

Fig. 11. Results of expansion block thermal model verification.

3.2. Expansion block tooling model

To validate the model in Sections 2.3 and 2.4, several Expansion Block Tool configurations where studied. The conditions were as follows: $\sigma = 620$ KPa, $E = 599$ MPa, $\nu = 0.3$, $\alpha = 140 \times 10^{-6}$ °C^{-1}, $\Delta T = 156$°C. As before, the required number of tows was calculated using Eq. (16) and model developed in Section 2.3. Verification of the model was determined by comparing the experimentally achieved rib dimensions with those predicted by Eqs. (9) and (10).

The experimental setup is shown in Fig. 10. No skin was used so that the achieved rib height could be accurately determined. For each expansion tool configuration tested, the predicted number of tows, T_n, was laid up into the tool. The material used was IM7/977-2 and was cured to the manufacture's recommended cure cycle.

All results of the experiments were in good agreement with the model. These are shown in Fig. 11, where the experimental rib widths are shown compared to those predicted by the theory. The largest difference between predicted and experimental dimensions was about 7% of the experimental rib width in that case.

4. Conclusion

Two tooling types, hybrid tooling and expansion block tooling, have recently been developed to produce high quality AGS structures. Both tooling types must be carefully sized to provide for good quality parts of the correct dimensions. Two separate thermal models have been developed to properly size these types of tooling. Using these models, the required tooling geometry can be related to the desired rib geometry and the necessary processing conditions (temperature and pressure). The models have been experimentally verified using data presented in this paper.

References

[1] Huybrechts S, Hahn S, Meink TE. Grid stiffened structures: a survey of fabrication, analysis and design methods. 1999 International Conference on Composite Materials (ICCM) Proceedings. 1999.

[2] Huybrechts S, Meink TE. Advanced grid stiffened structures for the next generation of launch vehicles. 1997 IEEE Aerospace Conference Proceedings. 1997.

[3] Meink TE, Gregoreck G. Composite grid vs. composite sandwich: a comparison based on payload shroud requirements. 1998 IEEE Aerospace Conference Proceedings. 1998.

[4] Meink TE, Huybrechts S. Hybrid tooling for advanced grid stiffened (AGS) structures. 1996 SAMPE Technical Conference Proceedings. 1996.

[5] Huybrechts S, Tsai SW. Analysis and behavior of grid structures. Compos Sci Technol 1996;56:1001–15.

[6] Cook R, Malkus D, Plesha M. Concepts and applications of finite element analysis. 3rd ed. New York: Wiley, 1989.